Theoretical Study of the Hydrogen Exchange Coupling in the Metallocene Trihydride Complexes $[(C_5H_5)_2MH_3]^{n+}$ (M = Mo, W, n = 1; M = Nb, Ta, n = 0)

Santiago Camanyes, Feliu Maseras, Miquel Moreno, Agustí Lledós,*
José M. Lluch,* and Juan Bertrán

Contribution from the Departament de Química, Universitat Autònoma de Barcelona, 08193 Bellaterra, Barcelona, Spain

Received August 8, 1995. Revised Manuscript Received March 1, 1996[⊗]

Abstract: The effect on the hydrogen exchange coupling in metallocene $[(C_5H_5)_2MH_3]^{n+}$ complexes under the substitution of the transition metal M is theoretically analyzed using a simple methodology that requires a modest number of ab initio electronic energy calculations that are used in a one-dimensional tunneling model within a basis set method. Concretely, the cases M = Mo, W (n = 1) and M = Nb, Ta (n = 0) whose hydrogen exchange couplings have been experimentally measured through the corresponding ^1H NMR spectra are considered. Our results of the exchange couplings at different temperatures for the considered cases are in satisfactory agreement (within the correct order of magnitude) with experimental results. This agreement seems to confirm that the mechanism we previously established for some formally d^4 iridium complexes that involved a dihydrogen-like transition state is also operative in the case of d^0 transition metal trihydride complexes. As a matter of fact, it is the stability of the η^2-H_2 structure relative to the minimum energy trihydride that is the main parameter governing the magnitude of the exchange coupling.

I. Introduction

It is now well-accepted that the unusual NMR proton spin couplings between labile hydride protons in transition metal trihydride complexes are due to quantum mechanical hydrogen exchange.[1−8] The occurrence of these exchange couplings, J_{exc}, leads, in some cases, to observed proton−proton couplings, J_{A-B}, which are considerably larger than magnetic couplings arising by the normal Fermi contact mechanism.

For iridium complexes, couplings of up to 1565 Hz have been observed.[1b] The magnitude of the coupling has been shown to be a sensitive function of the ligands attached to the metal and the observation temperature. This behavior was successfully analyzed by combining the construction of ab initio potential energy surfaces with a one-dimensional tunneling model using a basis set method.[7]

More recently Heinekey[9] has analyzed the effect of a change in the central transition metal on the exchange coupling. In particular, he has obtained the ^1H NMR spectra of the metallocene trihydride complexes $[(C_5H_5)_2MH_3]^{n+}$ (M = Mo, W (n = 1); M = Nb, Ta (n = 0)). For three of the considered cases (M = W, Nb, Ta), moderate values of the J_{A-B} coupling (7−20 Hz) are observed at room temperature consistent with an AB_2 spin system. Concretely, the complexes corresponding to W and Ta exhibit a proton coupling of 8.5 and 9.5 Hz, respectively, which are independent of the temperature in the range 203−303 K. Therefore, no significant exchange coupling was found for these two metallocenes. Conversely, for the Nb complex, a clear temperature dependence is obtained for the observed coupling that reduces with decreasing temperature, practically vanishes at 243 K, and then reappears at 173 K. This was attributed to a modest quantum mechanical exchange coupling, which is a sensitive function of temperature, so that it has a value of 26.4 Hz at 303 K, whereas it is zero at 173 K. On the other hand, the molybdenum complex presents an extremely large value of J_{A-B} (ca. 1000 Hz) at 203 K that decreases to 450 Hz at 153 K, this fact indicating the existence of an important exchange coupling.

The problem of quantum mechanical exchange coupling on $(C_5H_5)_2MH_3$ (M = Nb and Ta) trihydride complexes has been theoretically addressed by Daudey and co-workers[8a] using the Landesman's model, which is a crude approximation based on a hard-spheres potential, by taking the parameters from ab initio RHF calculations on the model system MCl_2H_3. Unfortunately, their results failed to reproduce the experimental evidence that the trihydride is the most stable structure for the Nb complex

---

[⊗] Abstract published in *Advance ACS Abstracts,* April 15, 1996.

[1] (a) Heinekey, D. M.; Payne, N. G.; Schulte, G. K. *J. Am. Chem. Soc.* **1988**, *110*, 2303. (b) Heinekey, D. M.; Millar, J. M.; Koetzle, T. F.; Payne, N. G.; Zilm, K. W. *J. Am. Chem. Soc.* **1990**, *112*, 909.

[2] (a) Jones, D. H.; Labinger, J. A.; Weitekamp, D. P. *J. Am. Chem. Soc.* **1989**, *111*, 3087. (b) Zilm, K. W.; Heinekey, D. M.; Millar, J. M.; Payne, N. G.; Demou, P. *J. Am. Chem. Soc.* **1989**, *111*, 3088. (c) Zilm, K. W.; Heinekey, D. M.; Millar, J. M.; Payne, N. G.; Neshyba, S. P.; Duchamp, J. C.; Szczyrba, J. *J. Am. Chem. Soc.* **1990**, *112*, 920. (d) Zilm, K. W.; Millar, J. M. *Adv. Magn. Reson.* **1990**, *15*, 163.

[3] (a) Antiñolo, A.; Carrillo, F.; Fernández-Baeza, J.; Otero, A.; Fajardo, M.; Chaudret, B. *Inorg. Chem.* **1992**, *31*, 5156. (b) Antiñolo, A.; Carrillo, F.; Chaudret, B.; Fajardo, M.; Fernández-Baeza, J.; Lanfranchi, M.; Limbach, H. H.; Maurer, M.; Otero, A.; Pellinghelli, M. A. *Inorg. Chem.* **1994**, *33*, 5163.

[4] (a) Heinekey, D. M.; Payne, N. G.; Sofield, C. D. *Organometallics* **1990**, *9*, 2643. (b) Arliguie, T.; Chaudret, B.; Jalón, F.; Otero, A.; López, J. A.; Lahoz, F. J. *Organometallics* **1991**, *10*, 1888. (c) Heinekey, D. M.; Harper, T. G. P. *Organometallics* **1991**, *10*, 2891.

[5] Antiñolo, A.; Chaudret, B.; Commenges, G.; Fajardo, M.; Jalón, F.; Morris, R. H.; Otero, A.; Schweltzer, C. T. *J. Chem. Soc., Chem. Commun.* **1988**, 1210.

[6] Gusev, D. G.; Kuhlman, R.; Sini, G.; Eisenstein, O.; Caulton, K. G. *J. Am. Chem. Soc.* **1994**, *116*, 2685.

[7] (a) Jarid, A.; Moreno, M.; Lledós, A.; Lluch, J. M.; Bertrán, J. *J. Am. Chem. Soc.* **1993**, *115*, 5861. (b) Jarid, A.; Moreno, M.; Lledós, A.; Lluch, J. M.; Bertrán, J. *J. Am. Chem. Soc.* **1995**, *117*, 1069.

[8] (a) Barthelat, J. C.; Chaudret, B.; Daudey, J. P.; DeLoth, P.; Poilblanc, R. *J. Am. Chem. Soc.* **1991**, *113*, 9896. (b) Limbach, H. H.; Scherer, G.; Maurer, M.; Chaudret, B. *Angew. Chem., Int. Ed. Engl.* **1992**, *31*, 1369. (c) Clot, E.; Leforestier, C.; Eisenstein, O.; Pélissier, M. *J. Am. Chem. Soc.* **1995**, *117*, 1797.

[9] Heinekey, D. M. *J. Am. Chem. Soc.* **1991**, *113*, 6074.

S0002-7863(95)02689-8 CCC: $12.00 © 1996 American Chemical Society

by obtaining a dihydrogen hydride complex 14.6 kcal/mol more stable than the trihydride form.

In a previous work[7] we theoretically studied at the MP2 level the effect of ligand substitution and temperature dependence on the hydrogen exchange coupling in $[(C_5H_5)Ir(L)H_3]^+$ complexes. The purpose of this paper is to provide a theoretical explanation of the effect on exchange coupling in the metallocene trihydride $[(C_5H_5)_2MH_3]^{n+}$ complexes under the substitution of the transition metal. Concretely, the cases M = Mo, W, Nb, and Ta, for which the ^{1}H NMR couplings have been evaluated from the corresponding spectra, will be analyzed. Moreover, we will try to test if the mechanism established for formally d^4 iridium complexes that involves a dihydrogen-like transition state can be extended to the case of d^0 transition-metal trihydride complexes. To this aim we will combine the construction of an ab initio Becke3LYP DFT potential energy surface with a realistic tunneling model.

II. Methodological Details

In what follows, subsection A describes the ab initio calculations that will be employed to explore the potential energy surface. Subsection B presents the tunneling model used in this paper.

A. Ab Initio Calculations. All calculations have been carried out with the GAUSSIAN 92/DFT[10] series of programs. The Density Functional Theory (DFT), which is reaching a widespread use in the field of theoretical transition metal chemistry,[11] was applied with a functional that seems to be nowadays one of the most used. The particular functional used was the Becke's three-parameter hybrid method[12] using the LYP correlation functional (Becke3LYP).[13]

An effective core potential operator has been used to replace core electrons of metal atoms.[14] This involved 28 electrons for the second-row transition metals (Nb and Mo) and 60 electrons for the third-row transition metals (Ta and W). The basis set used for the metal was that associated with the pseudopotential[14] with a standard valence double-ζ LANL2DZ contraction.[10] For the other atoms the valence double-ζ 6-31G basis set was used.[15] A polarization p shell was added to the hydrogen atoms[16] directly attached to the metal.

All along the exploratory process of the potential energy surface the (C_5H_5) fragments were restricted to a local C_{5v} symmetry.

B. Tunneling Model. In order to apply the tunneling model, a one-dimensional potential energy profile has to be defined. We have assumed that the mechanism is similar to the one we previously analyzed for the iridium complexes.[7]

The reaction path can be better envisaged by looking at Figure 1.

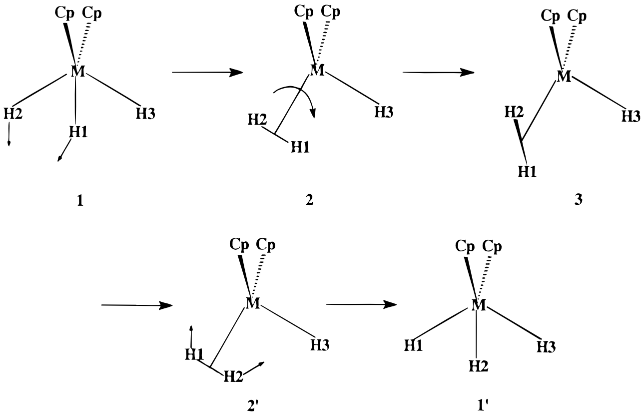

Figure 1. Proposed path for the hydrogen exchange mechanism in metallocene trihydride complexes.

Starting from the minimum energy structure (point **1** in Figure 1), a lengthening of the M−X distance (X stays at the midpoint of the H_1-H_2 segment) and a shortening of the H_1-H_2 distance takes place, eventually reaching point **2**. Then the H_1-H_2 rotation occurs in order to reach the transition state (point **3**). This second portion of the reaction path is tracked by the value of the rotational angle θ of the H_1-H_2 bond in the plane orthogonal to the M−X direction so that θ varies from 0° at point **2** to $\theta = 90°$ at point **3**. From here on, the motions are reversed, the path passing consecutively through points **2′** and **1′** that are the symmetric counterparts of points **2** and **1**. Point **1** has been located by full geometry optimization (only the C_5H_5 fragments geometry is restricted as stated in the previous subsection). Point **3** has been obtained by optimizing the H_1-H_2 and the M−X distances and the X−M−H_3 angle (as shown in Figure 1, H_3 is the nonexchanging hydrogen). The angle θ is fixed at 90°. The rest of the geometrical parameters are also kept fixed to the minimum energy structure values.

Finally, the structure of point **2** is obtained by fixing θ to 0°, and the H_1-H_2 distance to the value of the previously obtained point **3**. The remaining two parameters (M−X distance and X−M−H_3 angle) are then optimized.

Symmetric double wells have been built[17] by means of cubic spline functions fitted in such a way that the energy barrier coincides with the energy difference between points **3** and **1** (obtained as described in the previous paragraph) and the path length coincides with the value estimated as it is explained in what follows: in going from point **1** to point **3** (half of the total path length) only the exchanging hydrogen atoms move. The path length between points **1** and **2** is evaluated as the shortest distance (the linear one) between both structures. The evolution from point **2** to point **3** is fundamentally considered a rigid rotation, in such a way that the path length is approximated as twice (there are two exchanging hydrogen atoms) the semicircumference length whose diameter is the H_1-H_2 distance.

Because we are interested in the evaluation of the exchange coupling, we must obtain the vibrational states of the double well. For this purpose we have used a basis set methodology by taking a set of localized Gaussian functions which have the form:[18]

$$\chi_i = \left(\frac{\alpha}{\pi}\right)^{1/4} \exp\left[\frac{-\alpha}{2}(s - s_i)^2\right]$$

where α is an optimizable parameter and s_i values are equally spaced points along the coordinate space. Then, a variational calculation by using **n** functions provides the lowest **n** eigenvalues and eigenfunctions of the one-dimensional system. In particular, we have used 99 Gaussian functions throughout all the calculations. We have observed that a further increase in the number of basis functions does not appreciably modify the energies of the levels below the barrier.

III. Results and Discussion

The geometries of the four $[(C_5H_5)_2MH_3]^{n+}$ complexes considered are presented in Tables 1 to 4 where the main geometrical parameters are shown for M = Nb, Ta, Mo, and W, respectively.

The first column of the tables gives the minimum energy structure (**1** in Figure 1). Theoretical results are compared to the experimental values, when available,[19] in the next column. The two final columns give the geometries of points **2** and **3**

---

[10] Frisch, M. J.; Trucks, G. W.; Schlegel, H. B.; Gill, P. M. W.; Johnson, B. G.; Wong, M. W.; Foresman, J. B.; Robb, M. A.; Head-Gordon, M.; Replogle, E. S.; Gomperts, R.; Andrés, J. L.; Raghavachari, K.; Binkley, J. S.; González, C.; Martin, R. L.; Fox, D. J.; Defrees, D. J.; Baker, J.; Stewart, J. J. P.; Pople, J. A. *Gaussian 92/DFT*; Gaussian, Inc.: Pittsburgh, PA, 1993.

[11] Ziegler, T. *Chem. Rev.* **1991**, *91*, 651.

[12] Becke, A. D. *J. Chem. Phys.* **1993**, *98*, 5648.

[13] Lee, C.; Yang, W.; Parr, R. G. *Phys. Rev.* **1988**, *B 37*, 785.

[14] Hay, P. J.; Wadt, W. R. *J. Chem. Phys.* **1985**, *82*, 299.

[15] Hehre, W. J.; Ditchfield, R.; Pople, J. A. *J. Chem. Phys.* **1972**, *56*, 2257.

[16] Hariharan, P. C.; Pople, J. A. *Theor. Chim. Acta* **1973**, *28*, 213.

[17] Bosch, E.; Moreno, M.; Lluch, J. M.; Bertrán, J. *J. Chem. Phys.* **1990**, *93*, 5685.

[18] (a) Hamilton, I. P.; Light, J. *J. Chem. Phys.* **1986**, *84*, 306. (b) Makri, N.; Miller, W. H. *J. Chem. Phys.* **1987**, *86*, 1451.

[19] Wilson, R. D.; Koetzle, T. F.; Hart, D. W.; Kvick, Å.; Tipton, D. L.; Bau, R. *J. Am. Chem. Soc.* **1977**, *99*, 1775.

Table 1. Geometrical Parameters for Points **1**, **2**, and **3**, As Described in the Text, for the $(C_5H_5)_2NbH_3$ System

distances, Å	1	1 exp[a]	2	3
$M-H_1$	1.750	1.65	1.886	2.088
$M-H_2$	1.734	1.65	1.886	2.088
$M-H_3$	1.734	1.76	1.734	1.734
$H_1\cdots H_2$	1.771	1.77	0.762	0.762
$H_1\cdots H_3$	1.771	1.77	2.230	2.586
$H_2\cdots H_3$	3.036	3.04	2.759	2.586

[a] X-ray Data. From ref 19.

Table 2. Geometrical Parameters for Points **1**, **2**, and **3**, As Described in the Text, for the $(C_5H_5)_2TaH_3$ System

distances, Å, and angles, deg	1	1 exp[b]	2	3
$M-H_1$	1.754	1.775	1.851	2.044
$M-H_2$	1.742	1.769	1.851	2.044
$M-H_3$	1.742	1.777	1.742	1.742
$M-C^a$	2.452	2.393	2.452	2.452
$C-C^a$	1.431	1.421	1.431	1.431
$C-H^a$	1.078	1.084	1.078	1.078
$H_1\cdots H_2$	1.818	1.848	0.766	0.766
$H_1\cdots H_3$	1.818	1.856	2.250	2.568
$H_2\cdots H_3$	3.095	3.157	2.781	2.568
$\angle H_1MH_2$	62.66	62.8	23.9	21.6
$\angle H_1MH_3$	62.66	63.0	77.5	85.0
$\angle H_2MH_3$	125.33	125.8	101.4	85.0

[a] Averaged. [b] Neutron diffraction data. From ref 19.

Table 3. Geometrical Parameters for Points **1**, **2**, and **3**, As Described in the Text, for the $[(C_5H_5)_2MoH_3]^+$ System

distances, Å	1	2	3
$M-H_1$	1.669	1.811	1.954
$M-H_2$	1.653	1.811	1.954
$M-H_3$	1.653	1.653	1.653
$H_1\cdots H_2$	1.637	0.778	0.778
$H_1\cdots H_3$	1.637	2.061	2.399
$H_2\cdots H_3$	2.836	2.609	2.399

Table 4. Geometrical Parameters for Points **1**, **2**, and **3**, As Described in the Text, for the $[(C_5H_5)_2WH_3]^+$ System

distances, Å	1	2	3
$M-H_1$	1.687	1.786	1.931
$M-H_2$	1.672	1.786	1.931
$M-H_3$	1.672	1.672	1.672
$H_1\cdots H_2$	1.697	0.783	0.783
$H_1\cdots H_3$	1.697	2.093	2.411
$H_2\cdots H_3$	2.916	2.645	2.411

that show the evolution of the reaction path up to the maximum energy point **3**, as already explained in subsection II.B (see Figure 1).

Comparison with experimental results can only be done for M = Nb and Ta (Tables 1 and 2, respectively). Good agreement with our theoretical values is clearly seen. The accordance is better for the tantalum complex, where the experimental data come from neutron diffraction experiments, whereas the niobium complex experimental results have been obtained through X-ray diffraction methods which are subject to more severe errors, particularly it tends to severely underestimate the M−H distances.

Evolution of $M-H_1$, $M-H_2$, and H_1-H_2 distances along structures **1**, **2**, and **3** is consistent with the mechanism of the hydrogen exchange initially described by Limbach *et al.*[20] and which we have successfully applied for the iridium complexes.[7] That is, from the minimum energy structure an enlarging of the two M−H distances and a diminution of the H_1-H_2 distance takes place in order to ease the exchange. This motion corresponds to the evolution toward the formation of a hydrogen molecule bonded to the transition metal which is able to rotate in such a way that the tunneling path is relatively short and takes place through an energy barrier not too high.

Table 5. Energies Relative to the Minimum Energy Structure (**1**) and Path Lengths

metal	$\Delta E(\mathbf{2})^a$	$\Delta E(\mathbf{3})^a$	$s_{\mathbf{1}-\mathbf{2}}{}^b$	$s_{\mathbf{2}-\mathbf{3}}{}^b$	$s_{\text{total}}{}^b$
Nb	11.42	25.40	1.223	1.198	4.840
Ta	19.80	37.73	1.228	1.204	4.863
Mo	5.49	16.42	1.075	1.221	4.592
W	13.53	28.49	1.085	1.231	4.632

[a] In kcal/mol. [b] In amu$^{1/2}$ Å.

From an energetic point of view, Table 5 gives the energies of points **2** and **3**, relative to the minimum energy structure **1**, for the different cases considered. In all the cases the classical trihydride structure corresponds to the true minimum on the energy surfaces in agreement with the experiment and in contrast with the previous RHF calculations.[8a] Nonclassical dihydrogen structures (point **2**) are in all the cases higher in energy as seen in the first column of Table 5. It is also to be noted that this nonclassical structure does not correspond to an actual minimum of the whole surface, but it belongs to the reaction path of the hydrogen exchange process. As seen in the first column of Table 5, the difference in energy between this point and the minimum energy structure increases along the series Mo < Nb < W < Ta. This result is in concordance with previous calculations by Lin and Hall[21] on the relative stabilities of classical and nonclassical isomers of 18-electron polihydride transition metal complexes. They found that the classical hydrides are preferred for transition metal with more diffuse d orbitals. It is well-known that the diffuse nature of transition metal d orbitals increases from right to left and from top to bottom in the Periodic Table. The same trends are observed for the H_1-H_2 distances at the minimum energy structures **1**, which qualitatively correlate very well with the energy difference between the dihydrogen and trihydride structures.

The relative energy of structure **3** (second column of Table 5) gives the energy barriers for the hydrogen exchange within the reaction-path mechanism assumed in building up the one-dimensional potential energy profile needed in order to apply the tunneling model as described in subsection II.B. To further assess the feasibility of this mechanism, we obtained by full optimization (only the local symmetry of the C_5H_5 fragments was retained) the transition state corresponding to the hydrogen exchange process for the molybdenum case. The energy of this transition state was only 1.52 kcal/mol below the corresponding point **3** for the M = Mo case. Geometry of this transition state was also very similar to the one considered in order to obtain structure **3**. This result confirms that the transition state has a dihydrogen structure, thus validating the assumed reaction path.

It is also interesting to note that the ordering of energy barriers given in the second column of Table 5 follows the same trend as η^2-H_2 (point **2**, first column) structures previously discussed. Therefore, the energy gap between the nonclassical and the classical structures is already a clear indication of the relative difficulty of the whole hydrogen exchange process.

The third and fourth columns in Table 5 give the distances (in mass-weighted Cartesian coordinates) between the minimum and the dihydrogen structure, point **2**, and between point **2** and

---

[20] Limbach, H. H.; Scherer, G.; Maurer, M.; Chaudret, B. *Angew. Chem., Int. Ed. Engl.* **1992**, *31*, 1369.

[21] (a) Lin, Z.; Hall, M. B. *J. Am. Chem. Soc.* **1992**, *114*, 6102. (b) Lin, Z.; Hall, M. B. *Coord. Chem. Rev.* **1994**, *135*, 845.

[22] Curtis, M. D.; Bell, L. G.; Butler, W. M. *Organometallics* **1985**, *4*, 701.

Table 6. Values of the Exchange Coupling (in Hz) at Different Temperatures for the Four Metal Complexes

metal	150 K	200 K	300 K
Nb	6.1×10^{-2}	8.0×10^{-2}	3.5×10^{-1}
Ta	4.9×10^{-3}	4.9×10^{-3}	5.0×10^{-3}
Mo	6.9×10^{2}	9.0×10^{2}	2.0×10^{3}
W	1.5×10^{-2}	1.5×10^{-2}	1.8×10^{-2}

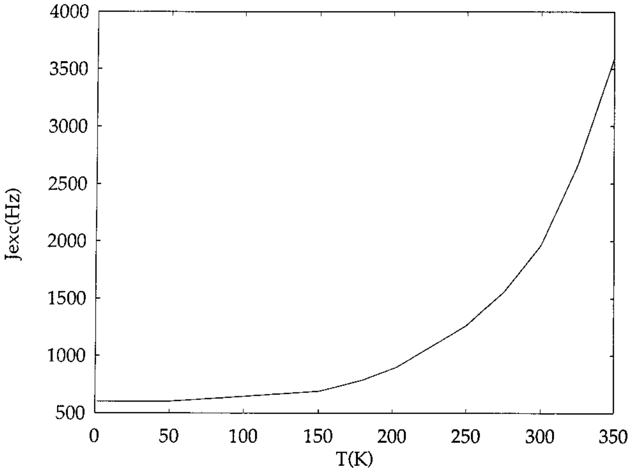

Figure 2. Temperature dependence of the exchange coupling for the $[(C_5H_5)_2MoH_3]^+$ complex.

the maximum energy point, point **3**. These distances were obtained with the simple method described in subsection II.B. Finally, the last column gives the total length of the reaction path between the two equivalent minima **1** and **1′**. It is obviously obtained by adding up the previous two columns and multiplying by two. It is noteworthy that the total distances follow a pattern parallel to the one already observed for the energy barriers, mainly due to the distances between points **1** and **2**; that is, the total path length increases when moving from right to left or from top to bottom along the Periodic Table. This fact is a consequence of the above-mentioned trend of diffuse character of d orbitals. This way molybdenum complex has the less diffuse orbitals, giving rise to the smallest H_1-H_2 distance at structure **1** and involving the shortest path length to reach the H_1-H_2 distance corresponding to structure **2**.

By using the data presented up to now we can already perform the tunneling calculations as explained in subsection II.B. These calculations provide the vibrational levels of the double well that appear in near-degenerate pairs. Since vibrational pairs are widely spaced, it may be assumed that the exchange process occurs independently in each pair. The energy difference between the lowest pair is a direct measure of the exchange coupling at zero Kelvin. At sufficient low temperature only this ground-state pair will be significantly occupied. As the temperature increases, the higher pairs become more populated. Because the transition rate from one vibrational state to another is expected to be very fast, the total exchange coupling can be obtained by a population-weighted average following a Boltzmann distribution over the thermally accessible pairs of vibrational states. All the levels with energy below the energy barriers are taken into account. Results at three specific temperatures for the four complexes studied are presented in Table 6. Figures 2 and 3 give in a more depictive way the dependence of the exchange coupling over a wide range of temperatures for the Mo and Nb complexes.

At this point, it should be emphasized that the exchange coupling is proportional to the tunneling rate. In this way, the dependence on the energy barrier is roughly exponential. As a consequence, exchange coupling is very sensitive to the precision with which the energy barrier is obtained. So, the theoretical J_{exc} values obtained in this work should be taken as an approximation that determines their order of magnitude. Even so, the values obtained are different enough to show clearly distinct behaviors of the four considered complexes.

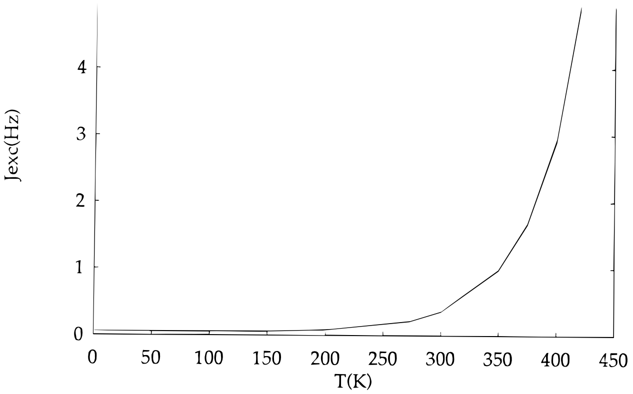

Figure 3. Temperature dependence of the exchange coupling for the $(C_5H_5)_2NbH_3$ complex.

The results shown in Table 6 and Figures 2 and 3 permit a classification of the exchange couplings in three categories. First of all, the Ta and W complexes show a negligible coupling exchange that is also quite temperature independent. This result is in accordance with the experimental findings. On the other hand, the Nb complex also has an almost zero exchange coupling at low temperature. This coupling, however, becomes higher as temperature increases. This behavior is again in accordance with the experimental NMR analysis presented in the introduction. Our theoretical model, however, predicts a more modest increase of exchange coupling with temperature than the one found by Curtis *et al.*[22] and Heinekey.[9] This error is likely to come from the use of a one-dimensional tunneling model that clearly exaggerates the energy difference between excited vibrational pairs leading therefore to theoretical $J_{exc}(T)$ curves that are less steep.

On the other hand, the exchange coupling values for the Mo case are orders of magnitude higher than for the other three metals. This was to be expected given the clearly lower energy barrier obtained for this case. The other magnitude that controls the coupling, the total length of the path, is also favorable. Comparison with experimental values at 153 and 203 K (450 and 1000 Hz, respectively) again shows excellent agreement.

So far, we have shown how similar the behavior of these d^0 metallocene complexes and the previously studied d^4 iridium complexes is. Certainly, in both cases the hydride exchange occurs through a dihydrogen-like transition state, which is reached through a similar reaction path. However, there is a significant difference between both cases. This is the relationship between the reaction barrier and the exchange coupling. We had found that for the $[(C_5H_5)Ir(L)H_3]^+$ complexes, a barrier of 14.1 kcal/mol was associated to an exchange coupling J_{exc} of 112.3 Hz ($L = PH_3$), while a barrier of 10.7 kcal/mol brought the value of J_{exc} to 1279.5 Hz. In contrast, for the $[(C_5H_5)_2MH_3]^{n+}$ complexes, we find that a barrier of 16.4 kcal/mol still has a J_{exc} value of 600.6 Hz (Mo) (these three exchange couplings correspond to a temperature of 0 K). This apparent shift in the dependence between the energy barrier and the exchange coupling cannot be explained by a difference in the total path length, which is actually also slightly longer for the d^0 species.

The explanation comes from the different shape of the energy profile in both types of reactions. Figure 4 shows the energy profile for one representative example of each system. The

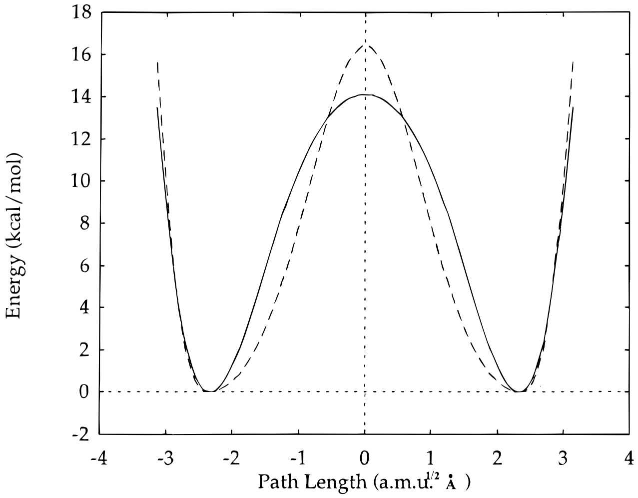

Figure 4. Schematic comparison of energy profiles for the hydride exchange in the $[(C_5H_5)Ir(PH_3)H_3]^+$ complex (solid line) and the $[(C_5H_5)_2MoH_3]^+$ complex (dashed line).

difference is clear in the picture. In the case of the d^0 complex, the energy increases very slowly from the minimum, and then it has a sharp increase relatively close to the transition state. Things were somehow more smooth in the case of the d^4 species. As a result, the barrier for the d^0 system, despite being higher, is thinner, and the resulting tunneling effect is of the same order.

The reasons for this behavior can be examined in detail by analyzing the chemical properties of the systems. In the first place, it has to be recognized that the sharp increase in the case of the d^0 complex happens after reaching point **2**, the in-plane dihydrogen complex. That is, the partition of the energy barrier (from **1** to **3**) in two parts (from **1** to **2** and from **2** to **3**) is completely different in both cases. This means that for the d^0 species, it is relatively easy to reach the dihydrogen-like species **2**, but then there is a high rotation barrier of this dihydrogen unit. This can be explained through molecular orbital analysis. The formation of the dihydrogen species decreases the oxidation state of the metal, which becomes d^2. As Hoffmann *et al.* have shown[23] the occupied d orbital in a d^2 $[(Cp)_2MH]$ fragment lies in a plane that contains the M$-$H bond length and is perpendicular to the straight line joining the two Cp centers. This orbital can back-donate to the σ^* of the H_2 fragment when the dihydrogen is placed in that plane. This is the case of point **2**. However, when the H_2 is rotated 90°, the σ^* orbital does not find any occupied d orbital in the metal to interact so that the back-donation is completely lost in complex **3**, which therefore has a remarkably high energy. Recent experimental findings support this analysis.[24] In these works it has been observed that the H_2 rotation in the $[(Cp)_2M(\eta^2\text{-}H_2)L]$ (M = Ta, Nb; L = several π acceptor ligands) complexes has a large rotational barrier (ca. 10 kcal/mol) as compared with the usual values in (η^2-H_2) complexes which are lower than 3.5 kcal/mol.[25] This situation is different from that of the previously studied d^4 iridium trihydride complexes,[7] as in that case there were always available occupied metal orbitals to back-donate to the dihydrogen unit in both d^6 species **2** and **3**. In accordance with that, the energy difference between **2** and **3** was clearly lower.

A point that deserves additional comments is the fact that the H_1-H_2 distance of **2** in the present paper is very short, suggesting at first glance a rather weak back-donation for this structure. However, it has to be remembered that point **2** is not obtained as a minimum energy structure but merely as an intermediate point along the tunneling path. It is obtained by rotating the H_1-H_2 bond of the previously located transition state keeping constant the H_1-H_2 distance. Indeed the full optimization of structure **2** increases the H_1-H_2 distance (as a consequence of the back-donation not present in **3**) but simultaneously leads to structure **1**, the actual minimum energy structure of the process. It has to be underlined that the main purpose of structure **2** is to define a short enough tunneling path that does not involve an excessive energy barrier. The tunneling path obtained in this way seems to be reasonable and is validated by comparison of the theoretical predictions with the experimental results.

In summary, we have shown that the difference in exchange coupling can be directly related to the height of the energy barrier when isoelectronic species are compared. But some care must be taken when the species are not isoelectronic, since other effects can be important. In other words, it is fair to make a comparison between $[(C_5H_5)Ir(PH_3)H_3]^+$ and $[(C_5H_5)Ir(CO)H_3]^+$, or between $(C_5H_5)_2NbH_3$ and $[(C_5H_5)_2MoH_3]^+$, but extrapolations cannot be carried out between the two different systems. Furthermore, we have shown that our method, despite all its approximations, is able to reproduce the subtle differences between both systems, and to explain them in a satisfactory way.

IV. Conclusions

In this paper we have studied the exchange coupling process in metallocene trihydride $[(C_5H_5)_2MH_3]^{n+}$ complexes where M = Mo, W ($n = 1$) and M = Nb, Ta ($n = 0$). A combination of ab initio calculations with a one-dimensional tunneling model using a basis set method has allowed us to obtain the hydrogen exchange coupling and its temperature dependence for the different transition metal complexes, in good agreement with the experimental results. We have assumed that for these d^0 transition metal complexes the exchange mechanism goes through a dihydrogen-like transition state which is very similar to the mechanism we previously found[7] for some iridium d^4 complexes. As a matter of fact, the stability of the η^2-H_2 structure relative to the minimum energy trihydride is the main parameter that governs the magnitude of the exchange coupling, so that the coupling is lower when the η^2-H_2 structures are less stable with respect to the trihydride complex. This agreement with the experimental results seems to validate the proposed mechanism for these metallocenes.

Finally, it has to be noted that within a simple calculation we have been able to predict quite well (within the correct order of magnitude) the hydrogen exchange couplings of a series of trihydride transition metal complexes.

Acknowledgment. Financial support for this work was provided by the Dirección General de Investigación Científica y Técnica DGICYT through projects PB89-0318, PB92-0613, and PB92-0621. Use of computational facilities by the Center of Parallelism of Barcelona, CEPBA, is also acknowledged.

JA952689R

---

[23] Lauer, J. W.; Hoffmann, R. *J. Am. Chem. Soc.* **1976**, *98*, 1729.

[24] (a) Sabo-Etienne, S.; Chaudret, B.; Abou el Makarim, H.; Barthelat, J.-C.; Daudey, J.-P.; Moïse, C.; Leblanc, J.-C. *J. Am. Chem. Soc.* **1994**, *116*, 9335. (b) Jalón, F. A.; Otero, A.; Manzano, B. R.; Villaseñor, E.; Chaudret, B. *J. Am. Chem. Soc.* **1995**, *117*, 10123. (c) Sabo-Etienne, S.; Chaudret, B.; Abou el Makarim, H.; Barthelat, J.-C.; Daudey, J.-P.; Ulrich, S.; Limbach, H.-H.; Moïse, C. *J. Am. Chem. Soc.* **1995**, *117*, 11602.

[25] Eckert, J.; Kubas, G. J. *J. Phys. Chem.* **1993**, *97*, 2378.